Inorganic Chemistry

Communication

pubs.acs.org/IC

A Cyanide-Bridged Molybdenum Bis(maleonitriledithiolate) Square

Moumita Bose,[†] Golam Moula,[†] and Sabyasachi Sarkar*[,‡]

[†]Department of Chemistry, Indian Institute of Technology, Kanpur, Kanpur 208016, Uttar Pradesh, India

[‡]Department of Chemistry, Bengal Engineering and Science University, Shibpur, Botanic Garden, Howrah 711103, West Bengal, India

Supporting Information

ABSTRACT: $[Et_4N]_2[Mo^{IV}O(mnt)_2]$ (mnt = maleonitriledithiolate) reacts, as a synthon, with Me_3SiCN under an acidic medium to produce the square complex $[Et_4N]_4[Mo_4(\mu\text{-}CN)_4(mnt)_8]$ (**1**) in high yield. Complex **1** shows strong antiferromagnetic interactions between adjacent Mo atoms in the cluster. The presence of redox-active mnt as a capping ligand strongly influences the magnetic property of **1**. The physicochemical properties of **1** have been rationalized by density functional theory level of calculations.

Cyanide-bridged transition-metal complexes are of considerable interest in contemporary coordination chemistry because of their magneto-optical, electrochemical, and photo-induced magnetic properties.[1,2] Among these, cyanide-bridged "molecular squares" are the subject of intense current interest because of their potential application in nanoscale devices and molecular machinery.[1,2] A tetranuclear cyclometalated iridium(III) complex coordinated with a fluorophoric polypyridyl ligand is shown to display luminescence.[3] Classically, cyanide ion is known to stabilize transition metals in different oxidation states and therefore lead to intriguing physicochemical properties.[1−4]

Prussian blue is the best studied cyano-bridged metal complex, and a range of transition metals have been used to build Prussian blue analogues.[1,2,5,6] Molybdenum as a second-row element has a few examples of such an assembly.[7] There are reports of heterometallic cyano-bridged molybdenum linked to different 3*d* transition elements.[1,2,7−9] However, there is dearth of cyanide-bridged square complexes only with molybdenum.[7a] The introduction of molybdenum into the Prussian blue analogue structure leads to enhancement of the bulk magnetic ordering temperature (T_N) resulting from the more diffuse higher energy valence *d* orbitals of the metal.[7b,9,10] The classical metal carbonyl complex such as $Mo(CO)_3(CH_3CN)_3$ has been used as the precursor to synthesize hexa- and tetranuclear molybdenum complexes, where each Mo center possesses octahedral geometry.[7a]

We use a bis(dithiolate)molybdenum complex framework to construct cyano-bridged tetrameric clusters containing trigonal-prismatic molybdenum displaying interesting physicochemical properties. The dithiolate ligand in the starting complex limits the number of cyano linkages formed between Mo centers to form a square. The cyano-bridged tetrameric bis(dithiolate) molybdenum cluster complex $[Et_4N]_4[Mo_4(\mu\text{-}CN)_4(mnt)_8]$ (**1**) is readily synthesized by using $[Et_4N]_2[Mo^{IV}O(mnt)_2]$ (mnt = maleonitriledithiolate) in the presence of excess Me_3SiCN upon acidification with methanesulfonic acid[11−13] (Scheme S1 in the Supporting Information, SI).

In complex **1**, each Mo center bridges two other neighboring Mo atoms through two linear bidentate cyanide bridges. The remaining coordination sites of each of the six-coordinate Mo centers are occupied by two bidentate mnt ligands, so that each Mo center of the tetranuclear core exhibits a slightly distorted trigonal-prismatic geometry. The space-filling model shows that **1** is bowl-shaped (Figure 1). The C and N atoms of the bridging

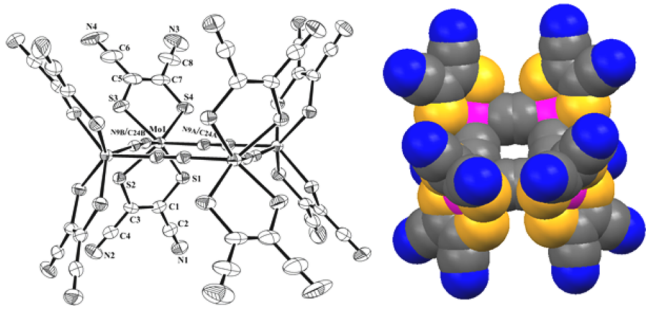

Figure 1. Left: ORTEP of the structure of the anion of **1**·$2CH_2Cl_2$ showing 50% probability thermal ellipsoids with a selected atom-labeling scheme. Right: Space-filling model of **1**.

cyanide are disordered, and each atom appears to be 0.5C/0.5N. The cyanide bridges in the tetranuclear assembly are almost linear, as is evident by the average Mo−N(C)−C(N) angle of 173.95(9)°. The disorder of C and N atoms in the bridged cyano group made crystallographic assignment of the oxidation state of Mo difficult. Because of its crystallization in the monoclinic *C*2/*m* space group, the tetramer (**1**) has been generated by growing the fragment unit $\{(C/N)(N/C)Mo(mnt)_2\}$; therefore, all of the fragment units of the tetramer are equivalent, and the oxidation level of the dithiolenes for each $\{Mo(mnt)_2\}$ unit is the same. In the assignment of electronic states for such $\{Mo(mnt)_2\}$ units, the oxidation state of the mnt ligand should be taken into account because the dithiolene ligand is redox-active.[14,15] In the neutral $[Mo(mnt)_3]$ complex, its electronic structure has been best described as $[Mo^{IV}(mnt^{\bullet-})_2(mnt^{2-})]$.[14] The coordinated dithiolenes in **1** have average C−S and C−C bond lengths of 1.731 and 1.364 Å, respectively. These bond lengths are in excellent agreement with the reported mixed oxidation states of the ligand mnt.[14] This suggests that each $\{Mo(mnt)_2\}$ unit

Received: August 23, 2013
Published: December 9, 2013

   dx.doi.org/10.1021/ic402160h | *Inorg. Chem.* 2014, 53, 6−8

present in **1** may have a ligand combination like $\{Mo^{III}(mnt^{\bullet-})(mnt^{2-})\}$ considering the overall charge of **1**. The spectroscopic, electrochemical, and magnetic data support that the mnt ligands in **1** are partially oxidized. Thus, **1** is formed by the combination of four equivalent $\{(C/N)(N/C)Mo^{III}(mnt^{\bullet-})(mnt^{2-})\}$ units (vide infra). The cyanide linkages with distinguishable C and N atoms are conventionally considered with the {−M−CN−M−NC−M−CN−M−NC−} assignment.[1−3] Molybdenum has equal affinity for the hard donor N and the soft donor C in lower oxidation states and therefore the other alternate arrangement of the cyanide linkage as {−Mo−CN−Mo−CN−Mo−CN−Mo−CN−} has been considered.[7a] Using this type of bridged cyanide frame, the formation of a tetranuclear core can be envisaged (Figure 1). The crystal packing of **1** along the *c* axis shows $p\pi(N)-d\pi(S)$ interaction of N and S of the coordinating mnt ligand between the two nearest tetrameric units (Figure S1 in the SI).[16] This leads to the formation of a 2D framework when viewed along the *c* axis (Figures S2 and S4 in the SI).

1 shows two prominent electronic absorptions (Figure S6 in the SI) at 560 and 399 nm, which may be attributed to the ligand-to-ligand charge-transfer transition[1d] characteristics to $\{Mo(mnt^{\bullet-})(mnt^{2-})\}$ systems,[14] suggesting the electronic state $\{Mo^{III}(mnt^{\bullet-})(mnt^{2-})\}$ in the $\{Mo(mnt)_2\}$ unit of **1**.[14,15,17] In solution, complex **1** is not very stable, and it slowly decomposes (Figure S6 in the SI).

The IR spectrum of **1** shows ν(CN) at 2210 and 2110 cm^{-1} related to the cyanide group in the mnt ligand[11−13] and to the bridging cyanide, respectively. One single ν(CN) stretch assigned for bridging cyanides states that **1** possesses one type of linkage like $\{Mo^{III}-CN-Mo^{III}\}$.

Each Mo center of **1** exhibits a trigonal-prismatic geometry. Hexacoordinated molybdenum(IV) complexes with such a geometry showed spin pairing of d^2 electrons resulting in diamagnetism.[18] The monomeric building unit of complex **1** is $\{Mo(CN)(mnt)_2\}$, devoid of a strong oxo group. The cyanide with its capability of mediating electronic interaction acts as the bridging group, leading to the tetrameric structure of **1**.

The magnetic behavior of compound **1** (Figures 2 and S7 in the SI) reveals strong antiferromagnetic coupling within the four $\{Mo^{III}(mnt^{\bullet-})(mnt^{2-})\}$ centers. Each of the Mo^{III} ion or the $mnt^{\bullet-}$ ligand has an unpaired electron ($S = {}^1/_2$). At 300 K, $\chi_M T$ is 1.1 $cm^3\ K^{-1}\ mol^{-1}$, which is well below the value predicted for four uncoupled Mo^{III} centers ($S = {}^1/_2$) or for the $Mo^{III}mnt^{\bullet-}$ radical pair ($S = 1$). An approximate fit to the variable-temperature magnetic data was obtained using an isotropic exchange Hamiltonian (eq 1, where all of the terms have their usual significance).[19] For this, due correction with a combination of diamagnetism and temperature-independent paramagnetism (TIP) is introduced. Assuming ferromagnetic interactions between metal-radical orbitals in the $Mo^{III}mnt^{\bullet-}$ radical pair, a four-spin model of the four triplets ($S = 1$) is considered (Figure S8 in the SI). This is due to the orthogonality of the planes containing molybdenum magnetic *d* orbitals and a delocalized π-electron cloud of the oxidized dithiolene (Figure S9 in the SI). Such metal−radical ferromagnetic interaction is already documented.[19]

$$\hat{H} = \sum_{\langle i,j \rangle} J_{i,j}(\hat{S}_i \hat{S}_j) - g\beta H \sum_i \hat{S}_i \qquad (1)$$

The solid line in Figure 2 thus represents the best fit of the data to eq 1 with $g = 1.64$, $J_1 = 195.95\ cm^{-1}$, $J_2 = -9\ cm^{-1}$, and $J_3 = 171.50\ cm^{-1}$ and with corrections due to (diamagnetism + TIP) $= -6.3 \times 10^{-4}\ cm^3\ mol^{-1}$ and magnetic impurities $= 3 \times 10^{-3}$. Strong intermolecular antiferromagnetic interaction (J_3) is possible because of the intermolecular $p\pi(N)-d\pi(S)$ interaction based on the crystallographic study (Figure S1 in the SI).[19] Also, the intramolecular antiferromagnetic interaction (J_1) is high because of the high-energy 4*d* orbitals of the Mo^{III} centers.[7b] The intramolecular diagonal interaction (J_2) is ferromagnetic. The temperature dependence in the magnetic moment associated with the paramagnetic impurity and spin−orbit coupling could possibly account for the poor quality of the fit at lower temperature. The strong magnetic coupling present in the system confirms that the adjacent Mo centers are not in the different spin state (high/low) with Mo^{IV} because strong coupling is not possible between paramagnetic (triplet Mo^{IV}) and diamagnetic (singlet Mo^{IV}) centers.[20] The resultant effective magnetic moment (μ_{eff}) 2.98 μ_B per tetramer at room temperature reveals an overall electronic spin of 2 in the molecular square of **1**.

Complex **1** shows two quasi-reversible oxidative waves at 0.60 and 0.41 V and a reductive wave at −1.03 V vs Ag/AgCl, respectively (Figure S10 in the SI). The oxidation waves may be assigned to oxidation of the ligand mnt and Mo^{III} centers, respectively, while the reduction wave can be attributed to reduction of the $mnt^{\bullet-}$ moiety.[14,15] Another reduction wave at a very negative potential, −1.9 V (Figure S10 in the SI), is due to reduction of the coordinating mnt^{2-} ligand.[21]

The solid-state and solution (frozen) X-band (120 K) EPR of complex **1** exhibit an axial signal with an average $\langle g \rangle$ value at 1.95 (Figure S11 in the SI), which is expected from trigonal-prismatic Mo^{III} ($S = {}^1/_2$).[22] This *g* (deviating from 2.000) value suggests that the net unpaired electron density is centered on Mo rather than on S of the dithiolenes.[11,14,15,23] A $\langle g \rangle$ value much below 2 may be attributed to the cyanide linkages, allowing partly a spin neutralization effect of the Mo *d* spin. The fine splitting in the EPR signal is due to the hyperfine interaction of ^{95}Mo and ^{97}Mo nuclei ($I = {}^5/_2$) with the electronic spin. The large hyperfine coupling constant (A_z) value is presumably due to sulfur ligation around the trigonal-prismatic molybdenum (Figure S11 and Table S3 in the SI).[15c]

Complex **1** is a blue-emitting material (Figure S12 in the SI) with a 0.26 ms lifetime in solution under ambient conditions. Emission occurs in the blue region with a 427 nm maximum, when excited with 238 nm ultraviolet light (Figure S12 in the SI). In contrast in the solid state, excitation at 238 nm does not show

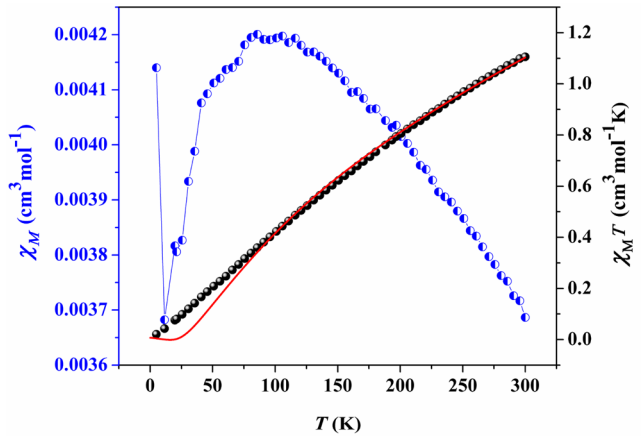

Figure 2. Magnetic behavior of complex **1** as measured in an applied field of 1000 G using a SQUID magnetometer. χ_M vs *T* (blue half-filled circles) and fitting (red line) on $\chi_M T$ vs *T* (black circles) of complex **1** in the solid state.

dx.doi.org/10.1021/ic402160h | Inorg. Chem. 2014, 53, 6−8

any emission. However, excitation around 560 nm results in **1** as a red-emitting material with a 0.05 ms lifetime under ambient conditions with several emission peaks in the red to far-red wavelength region with a 705 nm maximum (Figure S12 in the SI).

Density functional theory (DFT)[24] calculations of **1** revealed that the singly occupied molecular orbitals (SOMOs) and lowest unoccupied molecular orbitals (LUMOs) of **1** consist of both the ligand and metal orbitals (Figure S13 in the SI), thus confirming that the valence electronic states of complex **1** are composed of both the metal−ligand and metal−metal orbital interactions. Furthermore, DFT calculations show that the [−Mo−CN−Mo−CN−Mo−CN−Mo−CN−] linkage is more favorable compared to [−Mo−CN−Mo−NC−Mo−CN−Mo−NC−] because the SOMOs are more stable in the former compared to those in the latter (Figure S13 in the SI). The LUMO and LUMO+1 of complex **1** with the [−Mo−CN−Mo−CN−Mo−CN−Mo−CN−] linkage are almost similar in energy, and the orbital distribution is also similar but with alternate Mo centers (Figure S13 in the SI). This suggests that all of the Mo centers are basically under similar electronic environments, as manifested by the crystallographically imposed symmetry with the fragment unit $\{(C/N)(N/C)Mo(mnt)_2\}$ to build **1**.

dThe present work describes a neat and effective high-yield synthesis of a cyanide-bridged tetranuclear bis(dithiolate) complex (**1**) introducing a new synthon, $[Mo^{IV}O(mnt)_2]^{2-}$. Although Mo exists in the synthon in the IV oxidation state, the noninnocence of dithiolene leads to a cyanide-bridged reduced $[Mo^{III}(mnt^{\bullet-})(mnt^{2-})]$ framework consistent with the magnetic, spectroscopic, and electrochemical properties, which is further supported by the information obtained by DFT calculations.

■ ASSOCIATED CONTENT

Supporting Information

X-ray crystallographic data in CIF format, materials, methods, details of synthesis, analytical data, and computational details of **1**. This material is available free of charge via the Internet at http://pubs.acs.org.

■ AUTHOR INFORMATION

Corresponding Author

*E-mail: abya@iitk.ac.in or protozyme@gmail.com.

Notes

The authors declare no competing financial interest.

■ ACKNOWLEDGMENTS

M.B. and G.M. thank CSIR, New Delhi, for fellowships, and S.S. thanks DST, New Delhi, for funding. We thank Dr. Kuntal Pal to solve the disorder in the crystal structure. We also thank Dr. Hirofumi Yoshikawa and Kazuki Tanifuji from the Chemistry Department, Nagoya University, Japan, for helping us to collect the powder X-ray data.

■ REFERENCES

(1) (a) Verdaguer, M.; Bleuzen, A.; Marvaud, V.; Vaissermann, J.; Seuleiman, M.; Desplanches, C.; Scuiller, A.; Train, C.; Garde, R.; Gelly, G.; Lomenech, C.; Rosenman, I.; Veillet, P.; Cartier, C.; Villain, F. *Coord. Chem. Rev.* **1999**, *190−192*, 1023−1047. (b) Dunbar, K. R.; Heintz, R. A. *Prog. Inorg. Chem.* **1997**, *45*, 283−373. (c) Rombaut, G.; Verelst, M.; Golhen, S.; Ouahab, L.; Mathoniére, C.; Kahn, O. *Inorg. Chem.* **2001**, *40*, 1151−1159. (d) Nihei, M.; Sekine, Y.; Suganami, N.; Nakazawa, K.; Nakao, A.; Nakao, H.; Murakami, Y.; Oshio, H. *J. Am. Chem. Soc.* **2011**, *133*, 3592−3600.

(2) (a) Leininger, S.; Olenyuk, B.; Stang, P. J. *Chem. Rev.* **2000**, *100*, 853−908. (b) Schelter, E. J.; Karadas, F.; Avendano, C.; Wernsdorfer, W.; Dunbar, K. R. *J. Am. Chem. Soc.* **2007**, *129*, 8139−8149. (c) Qian, K.; Huang, X-. C.; Zhou, C.; You, X.-Y.; Dunbar, K. R. *J. Am. Chem. Soc.* **2013**, *135*, 13302−13305. (d) Karadas, F.; Schelter, E. J.; Schatruk, M.; Prosvirin, A. V.; Bacsa, J.; Smirnov, D.; Ozarowski, A.; Krzystek, J.; Telser, J.; Dunbar, K. R. *Inorg. Chem.* **2008**, *47*, 2074−2082.

(3) Baranoff, E.; Orselli, E.; Allouche, L.; Censo, D. D.; Scopelliti, R.; Grätzel, M.; Nazeeruddin, M. K. *Chem. Commun.* **2011**, *47*, 2799−2801.

(4) Sharpe, A. G. *The Chemistry of Cyano Complexes of the Transition Metals*; Academic Press: London, 1976.

(5) (a) Klausmeyer, K. K.; Wilson, S. R.; Rauchfuss, T. B. *Angew. Chem., Int. Ed.* **1998**, *37*, 1694−1696. (b) Heinrich, J. L.; Berseth, P. A.; Long, J. R. *Chem. Commun.* **1998**, 1231−1232.

(6) Holliday, B. J.; Mirkin, C. A. *Angew. Chem., Int. Ed.* **2001**, *40*, 2022−2043.

(7) (a) Contakes, S. M.; Rauchfuss, T. B. *Angew. Chem., Int. Ed.* **2000**, *39*, 1984−1986. (b) Beauvais, L. G.; Long, J. R. *J. Am. Chem. Soc.* **2002**, *124*, 2110−2111. (c) Bell, A.; Lippard, S. J.; Roberts, M.; Walton, R. A. *Organometallics* **1983**, *2*, 1562−1572. (d) Pérez, J.; Hevia, E.; Riera, L.; Riera, V.; García-Granda, S.; García-Rodríguez, E.; Miguel, D. *Eur. J. Inorg. Chem.* **2003**, 1113−1120. (e) Contakes, S. M.; Rauchfuss, T. B. *Chem. Commun.* **2001**, 553−554.

(8) Mallah, T.; Auberger, C.; Verdaguer, M.; Veillet, P. *J. Chem. Soc., Chem. Commun.* **1995**, 61−62.

(9) See the SI.

(10) Sokol, J. J.; Hee, A. G.; Long, J. R. *J. Am. Chem. Soc.* **2002**, *124*, 7656−7657.

(11) Das, S. K.; Chaudhury, P. K.; Biswas, D.; Sarkar, S. *J. Am. Chem. Soc.* **1994**, *116*, 9061−9070.

(12) Majumdar, A.; Pal, K.; Sarkar, S. *J. Am. Chem. Soc.* **2006**, *128*, 4196−4197.

(13) Nagrajan, K.; Joshi, H. K.; Chaudhury, P. K.; Pal, K.; Cooney, J. A.; Enemark, J. H.; Sarkar, S. *Inorg. Chem.* **2004**, *43*, 4532−4533.

(14) Sproules, S.; Banerjee, P.; Weyhermüller, T.; Yan, Y.; Donahue, J. P.; Wieghardt, K. *Inorg. Chem.* **2011**, *50*, 7106−7122.

(15) (a) Begum, A.; Moula, G.; Sarkar, S. *Chem.—Eur. J.* **2010**, *16*, 12324−12327. (b) Begum, A.; Moula, G.; Bose, M.; Sarkar, S. *Dalton Trans.* **2012**, *41*, 3536−3540. (c) Bose, M.; Moula, G.; Begum, A.; Sarkar, S. *Inorg. Chem.* **2011**, *50*, 3852−3854.

(16) Stein, C. A.; Baker, A. D.; Lewis, N. A.; White, P. S. *J. Chem. Soc., Dalton Trans.* **1984**, 2073−2075.

(17) Shupack, S. I.; Billig, E.; Clark, R. J. H.; Williams, R.; Gray, H. B. *J. Am. Chem. Soc.* **1964**, *86*, 4594−4602.

(18) Stiefel, E. I.; Bennet, L. E.; Dori, Z.; Crawford, T. H.; Simo, C.; Gray, H. B. *Inorg. Chem.* **1970**, *9*, 281−286.

(19) See the SI.

(20) Li, F.; Clegg, J. K.; Goux-Capes, L.; Chastanet, G.; D'Alessandro, D. M.; Létard, J. F.; Kepert, C. J. *Angew. Chem., Int. Ed.* **2011**, *50*, 2820−2823.

(21) (a) Bose, M.; Moula, G.; Sarkar, S. *Chem. Biodiversity* **2012**, *9*, 1867−1879. (b) Moula, G.; Bose, M.; Datta, H.; Sarkar, S. *Polyhedron* **2013**, *52*, 900−908. (c) Moula, G.; Bose, M.; Sarkar, S. *Inorg. Chem.* **2013**, *52*, 5316−5327.

(22) (a) Rossman, G. R.; Tsay, F. D.; Gray, H. B. *Inorg. Chem.* **1973**, *12*, 824−829. (b) Krueger, S. T.; Poli, R.; Rheingold, A. L.; Staley, D. L. *Inorg. Chem.* **1989**, *28*, 4599−4607. (c) For octahedral Mo^{III} ($S = {}^3/_2$), additional peak at $g = 4$ is usually observed. For example, see: Averill, B. A.; Orme-Johnson, W. H. *Inorg. Chem.* **1980**, *19*, 1702−1705.

(23) See the SI.

(24) See ref 8 in the SI.